
Figures and figure supplements

Evaluation of Gremlin-1 as a therapeutic target in metabolic dysfunction-associated steatohepatitis

Paul Horn et al.

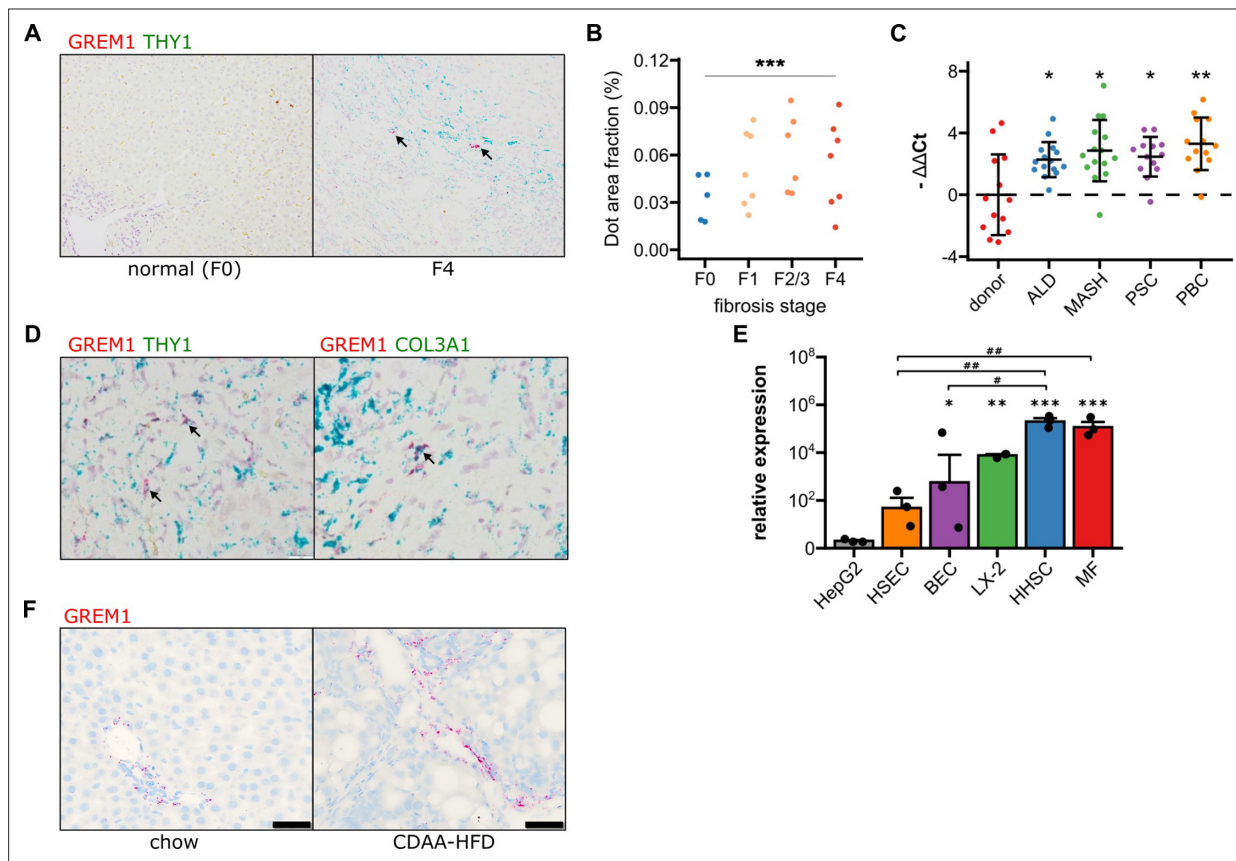


Figure 1. Validation of GREM1 expression in human and rat MASH liver fibrosis. **(A)** Representative RNAscope in situ hybridisation (ISH) images for co-staining of GREM1 (red) and THY1 (green) in normal human liver and MASH fibrosis. **(B)** Quantification of ISH staining areas across different stages of liver fibrosis. Significance was assessed by two-sided Jonckheere-Terpstra test ($***P=1.3 \times 10^{-09}$). **(C)** Quantification of human GREM1 qPCR across chronic liver diseases of different aetiology. Data are given as mean $-\Delta\Delta Ct \pm SD$, relative to donor liver and normalised to the expression of SRSF4, HPRT1, and ERCC3. Significance was assessed by multiple two-sided Welch t-test against donor control, followed by Bonferroni-Holm adjustment ($*P<0.05$, $**P=0.004$). **(D)** Representative histological images of RNAscope in situ hybridisation (ISH) for co-staining of GREM1 (red) and THY1 or COL3A1 (green) in MASH fibrosis. Representative double positive cells are indicated by arrows. **(E)** Quantification of qPCR for GREM1 mRNA in major primary human non-parenchymal cell types. HSEC – human sinusoidal endothelial cells, BEC – biliary epithelial cells, HHSC – human hepatic stellate cells, MF – myofibroblasts. **(F)** Representative RNAscope in situ hybridisation (ISH) images for GREM1 (red) in rats fed a standard chow or CDAA-HFD for 12 weeks.

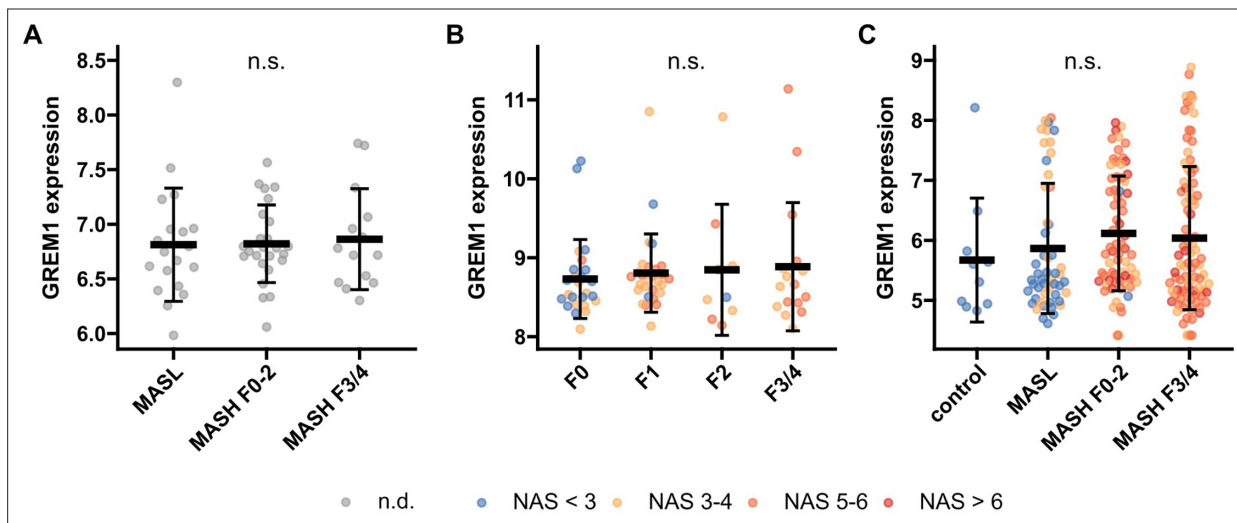


Figure 1—figure supplement 1. GREM1 gene expression in public bulk RNAseq data from human MASLD liver. (A) E-MTAB-9815 (n=58). (B) GSE130970 (n=78). (C) GSE135251 (n=216). All data are given as individual data points and mean \pm SD of variance stabilised expression as obtained from the vst function in DESeq2. n.s. – not significant, statistical significance was tested using the likelihood ratio test and Benjamini Hochberg correction in DESeq2.

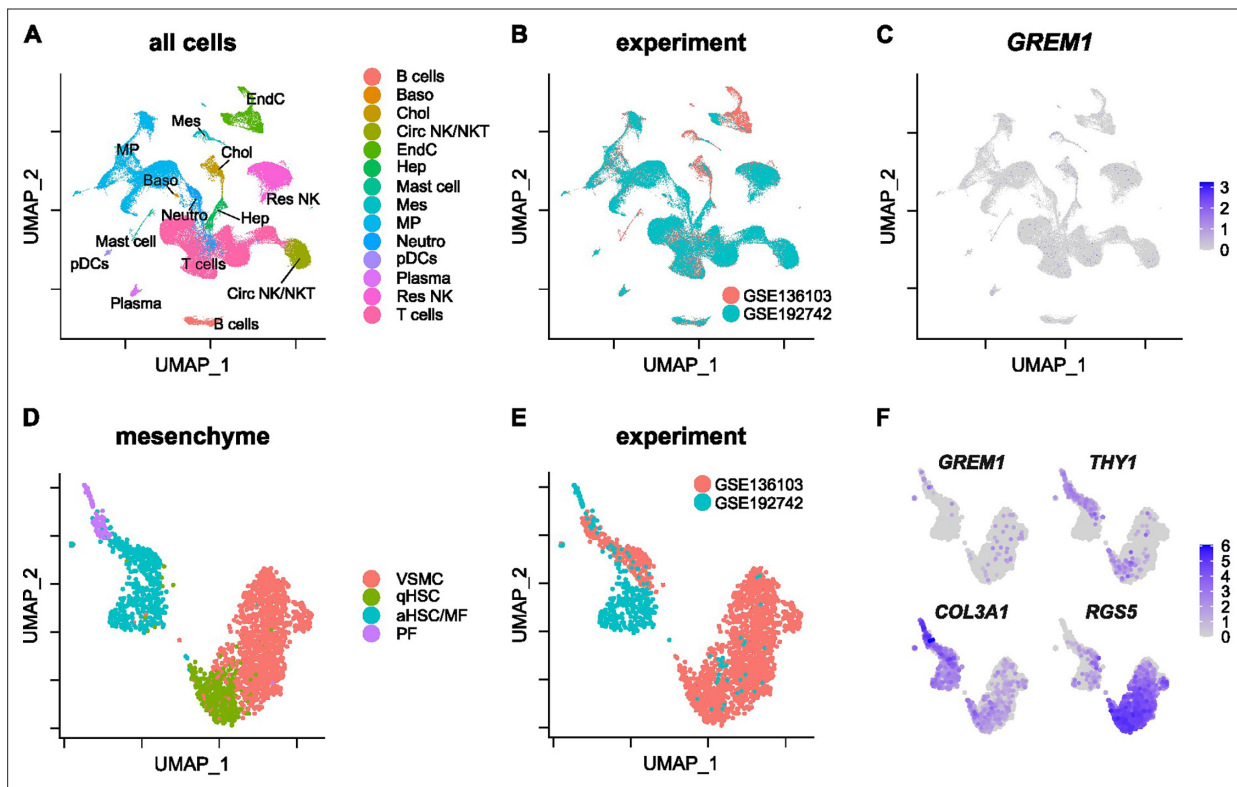


Figure 1—figure supplement 2. *GREM1* expression in publicly available human scRNA-seq data. **(A)** UMAP representation of all cells in GSE136103 and GSE192742 scRNA-seq datasets. Cells are coloured by cell type identity. **(B)** UMAP representation of all cells in GSE136103 and GSE192742 scRNA-seq datasets. Cells are coloured by experiment. **(C)** Log2-normalised *GREM1* gene expression in all cells. **(D)** UMAP representation of mesenchymal cells in GSE136103 and GSE192742 scRNA-seq datasets. Cells are coloured by cell cluster identity. **(E)** UMAP representation of mesenchymal cells in GSE136103 and GSE192742 scRNA-seq datasets. Cells are coloured by experiment. **(F)** Log2-normalised gene expression of *GREM1*, *THY1*, *COL3A1* and *RGS5* in mesenchymal cells.

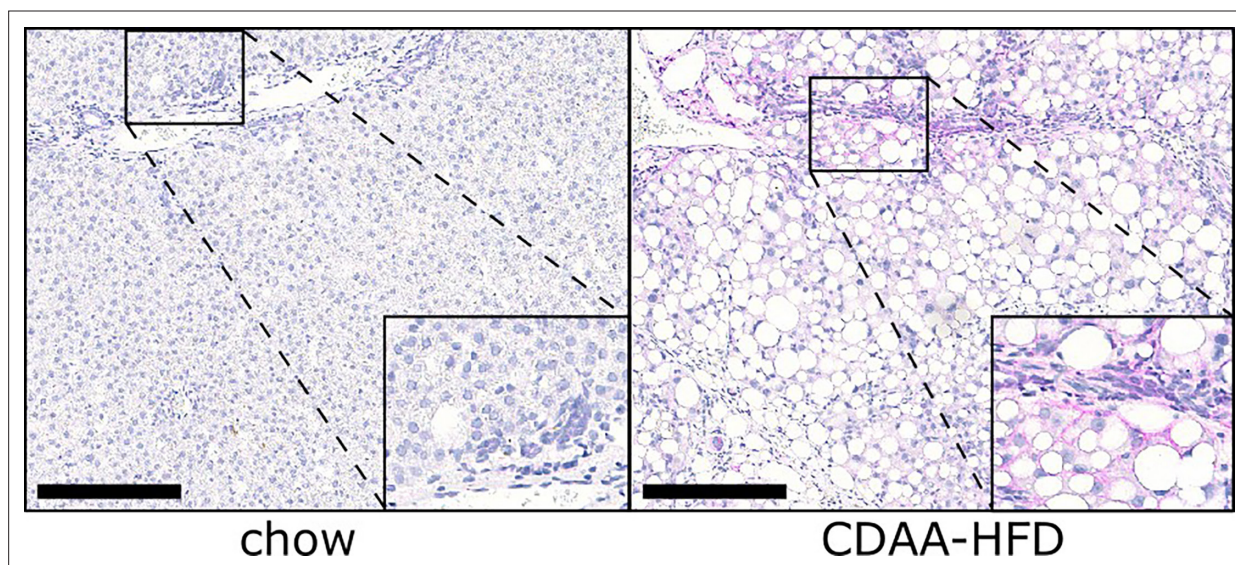


Figure 1—figure supplement 3. Representative immunohistochemistry images for GREM1 (red) in rats fed a standard chow or CDAA-HFD for 12 weeks. Inserts show zoomed in periportal/fibrotic areas. The size bar represents 250 μ m.

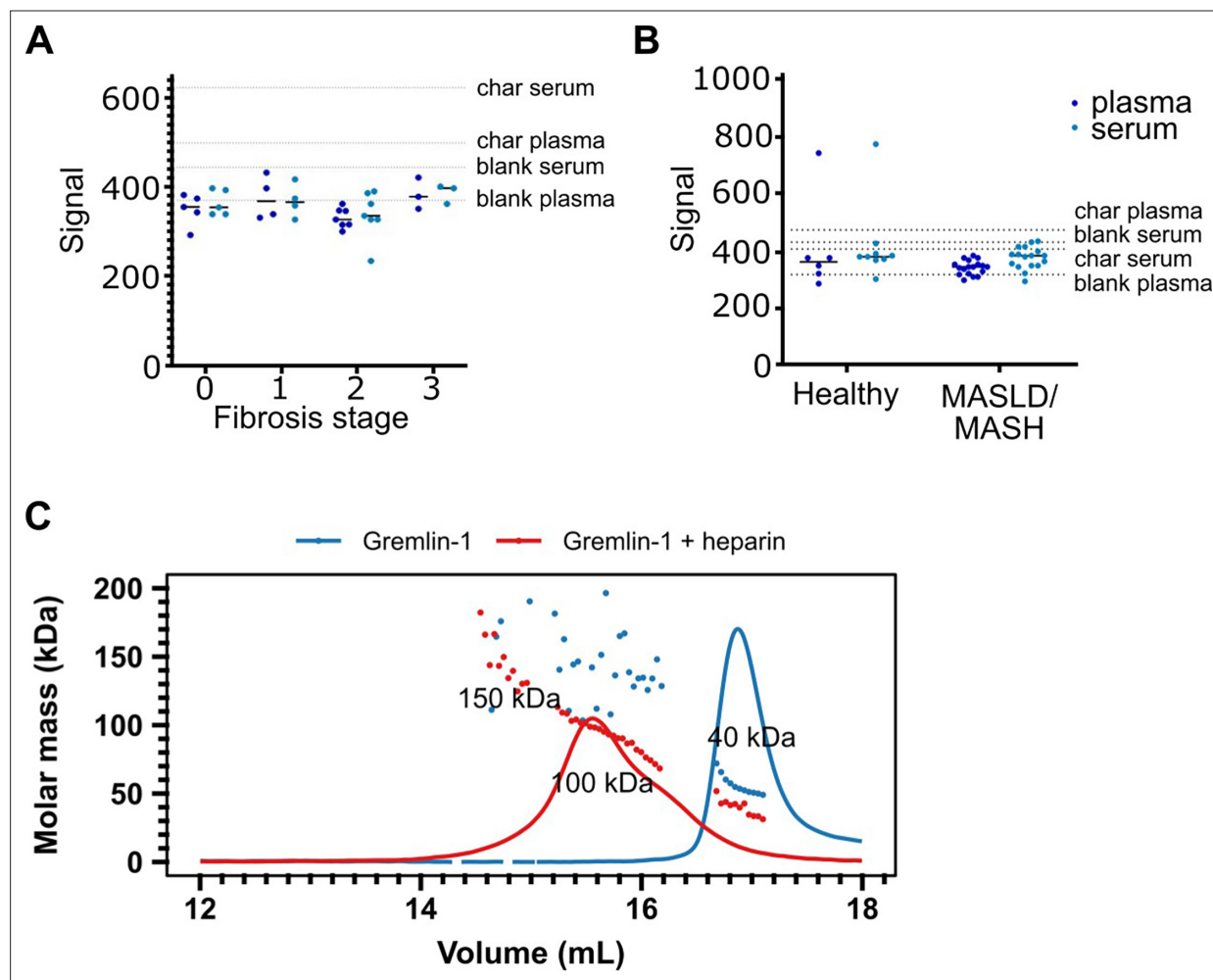


Figure 2. Circulating Gremlin-1 and evidence for heparin-binding. **(A)** Signal for Gremlin-1 protein in the LOCI assay in serum or plasma of MASH patients at different stages of fibrosis. Char serum/plasma – charcoal stripped serum/plasma. **(B)** Signal for Gremlin-1 protein in the LOCI assay in serum or plasma of healthy controls and MASLD/MASH. Data in A and B are given as single data points and median of luminescence signal. Dotted horizontal lines correspond to signal measured in control matrices, as given in text annotations. **(C)** Size exclusion chromatography for Gremlin-1 and heparin. Either gremlin-1 or gremlin-1 +heparan sulphate were run on a size exclusion chromatography column. The graph shows UV signal (continuous line) and estimated molar mass (points) on the y-axis depending on the eluting volume given on the x-axis. Text annotations give the estimated molar mass corresponding to each peak.

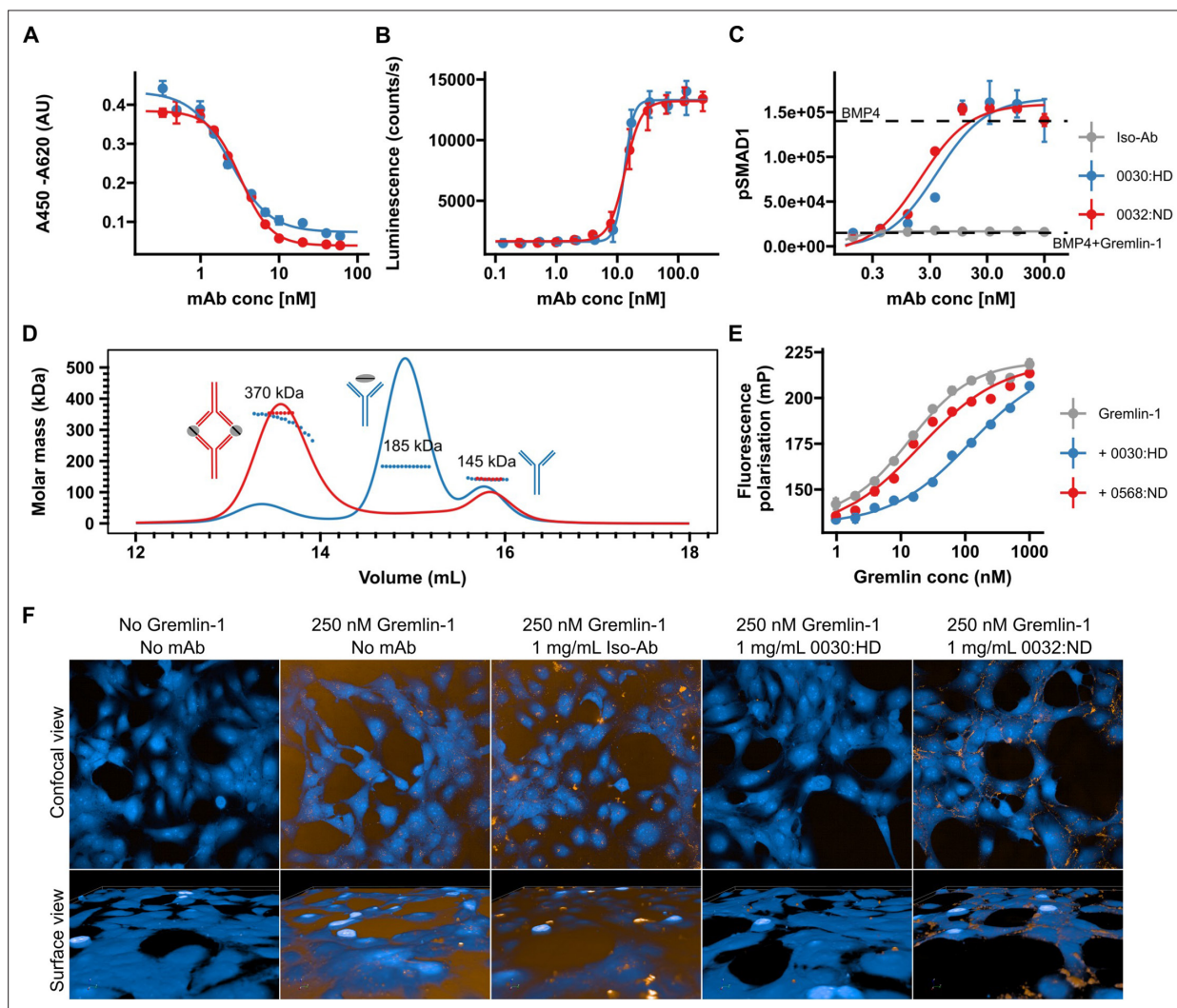


Figure 3. Validation of human recombinant anti-Gremlin-1 antibodies. Gremlin-1/BMP4 inhibition ELISA, measuring aG1-Ab ability to inhibit Gremlin-1 binding to BMP4. Higher absorbance indicates more Gremlin-1 binding to BMP4. $IC_{50}=2.7-3.1 \times 10^{-9}$ M. Dots and error bars represent mean \pm SD and lines show fitted four parameter log-logistic curve. **(A)** C2C12 BMP-responsive element Luc reporter gene assay. Luminescence is plotted over response to serial dilutions of anti-Gremlin-1 antibodies with higher luminescence indicating increased BMP4 activity. Dots and error bars represent mean \pm SD and lines show fitted four parameter log-logistic curve. $EC_{50}=1.27-1.36 \times 10^{-8}$ M. **(B)** SMAD1 phosphorylation on LX-2 cells treated with either BMP4, BMP4 and Gremlin-1 or BMP4, Gremlin-1 and serial dilutions of therapeutic antibody. Dots and error bars represent mean \pm SD and lines show fitted four parameter log-logistic curve. K_D [0032]=2.04 nM, K_D [0030]=3.96 nM. **(C)** Size-exclusion chromatography for Gremlin-1 in combination with heparin-displacing (0030) or non-heparin-displacing (0032) anti-Gremlin-1 antibody. The graph shows UV signal (continuous line) and estimated molar mass (points) on the y-axis depending on the eluting volume on the x-axis. Text annotations give the estimated molar mass corresponding to each peak. **(D)** Fluorescence polarisation heparin-binding assay. Serial dilutions of Gremlin-1 were incubated with fixed amounts of fluorescein-heparin sulfate and 1.5-fold molar excess anti-Gremlin-1 antibody. Increased fluorescence indicates reduced mobility of heparin molecules. Dots and error bars represent mean \pm SD and lines show fitted four parameter log-logistic curve. K_D [Grem1]=13.54 nM, K_D [0032]=19.56 nM and K_D [0030]=118.65 nM. **(E)** Gremlin-1 cell association assay. The upper panel shows a confocal view and the lower panel a three-dimensional cell surface view for Atto-532-labelled Gremlin-1 (yellow) on LX-2 cells (labelled with CellMask Blue). Representative images for different combinations of 250 nM Gremlin-1 and isotype or anti-Gremlin-1 antibodies are given.

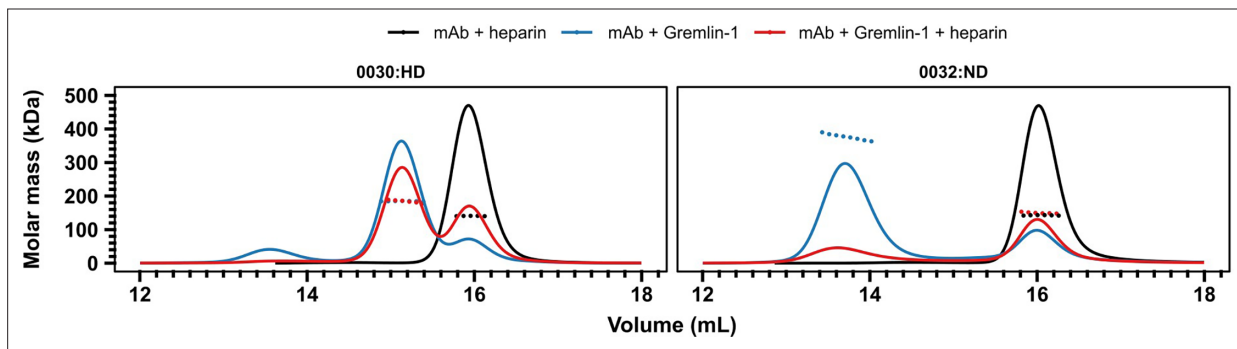


Figure 3—figure supplement 1. Size-exclusion chromatography for Gremlin-1-anti-Gremlin-1-heparin complexes. Different combinations of heparin-displacing ('0030, left) or non-displacing ('0032, right) therapeutic anti-Gremlin-1 antibodies with heparin alone, Gremlin-1 alone or Gremlin-1 and heparin were run on a size exclusion chromatography column. The graph shows UV signal (continuous line) and estimated molar mass (points) on the y-axis, depending on the eluting volume on the x-axis. The low recovery of 0032/Gremlin-1/heparin complexes was accompanied by visual precipitation in the sample vial, indicating the formation of macroscopic insoluble complexes.

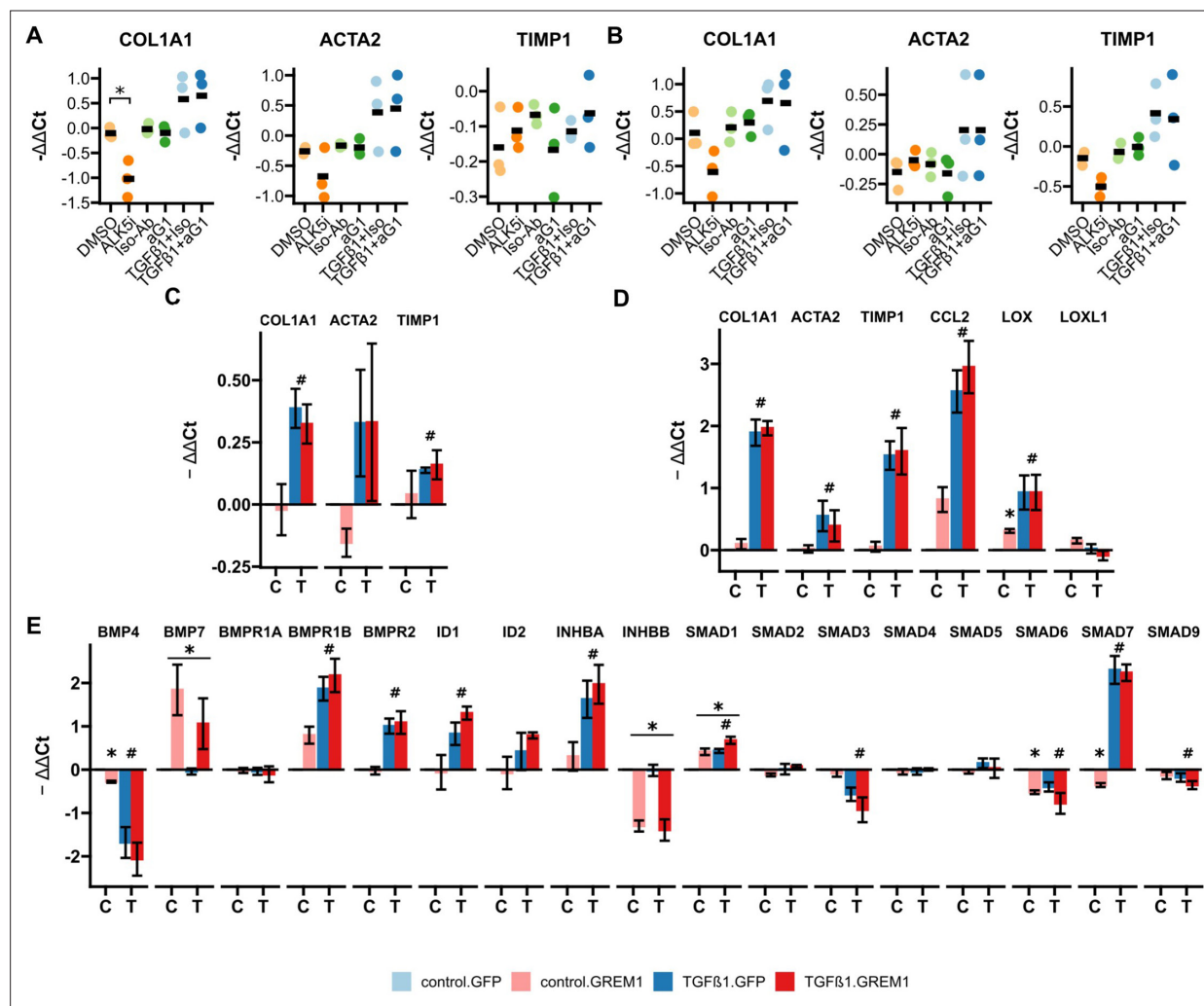


Figure 4. RTqPCR results for anti-Gremlin-1 and lenti-GREM1-treated fibrogenic cells. **(A)** Fibrogenic marker genes in primary human hepatic stellate cells treated with anti-Gremlin-1 (aG1) or isotype control antibodies (iso-Ab). **(B)** Fibrogenic marker genes in primary human hepatic myofibroblasts treated with anti-Gremlin-1 or isotype control antibodies. **(C)** Fibrogenic gene expression in lentivirally transduced HHSC. **(D)** Fibrogenic gene expression in lentivirally transduced LX-2. **(E)** BMP signalling related gene expression in lentivirally transduced LX-2. **(A–B)** Data are presented as individual data points and mean for $-\Delta\Delta\text{Ct}$ relative to untreated control and normalised to the expression of SRSF4. $*P < 0.05$ in One-Way ANOVA and *post-hoc* paired t-tests for pre-defined comparisons with Bonferroni-Holm adjustment. **(C–E)** Data are given as mean \pm SEM of $-\Delta\Delta\text{Ct}$ relative to GFP and vehicle control and normalised to the expression of SRSF4. $*P < 0.05$ in GREM1 vs GFP-control, $\#P < 0.05$ in TGF β 1 vs vehicle control in repeated measures Two-way ANOVA and *post-hoc* paired t-test for pre-selected comparisons and Bonferroni-Holm adjustment.

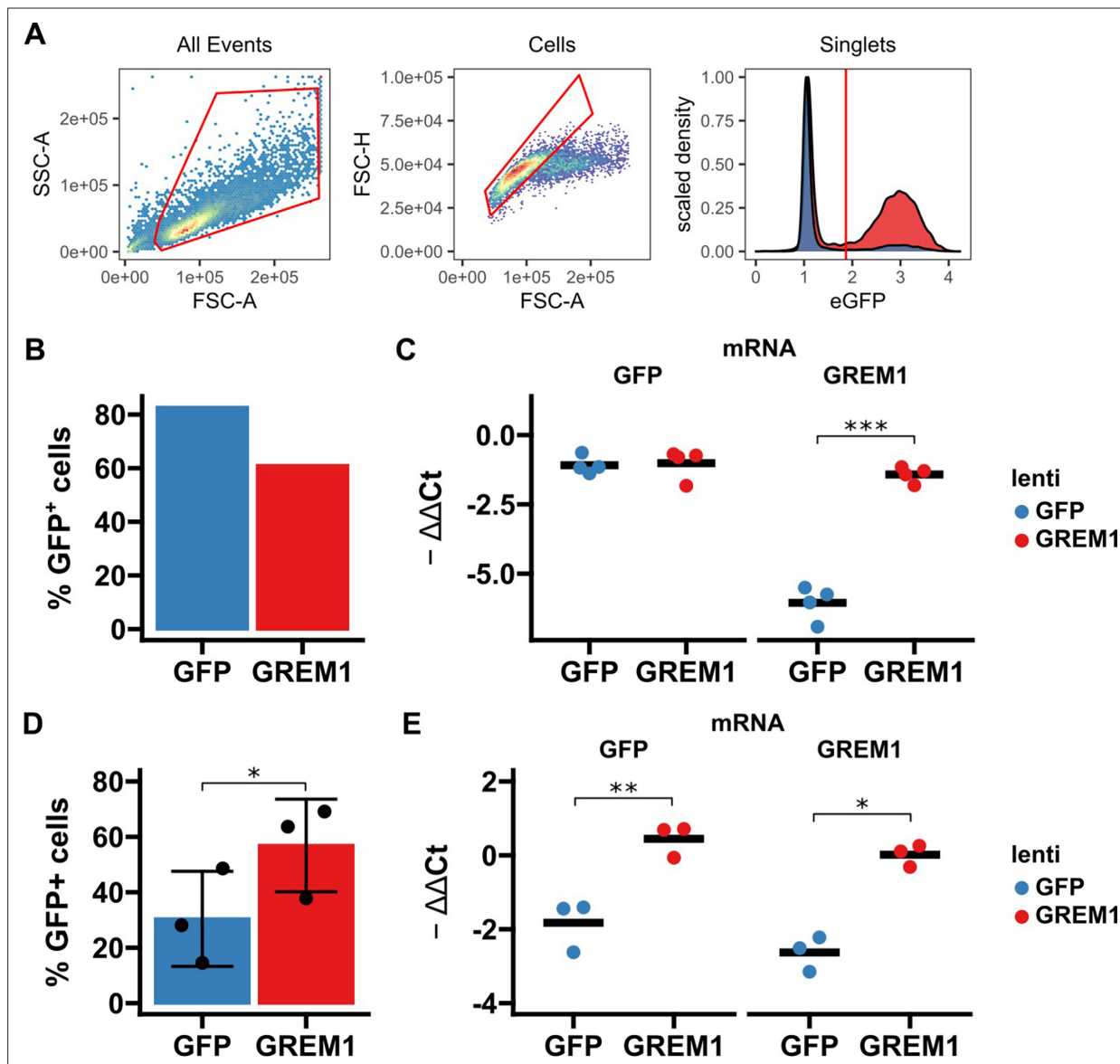


Figure 4—figure supplement 1. Validation of GREM1 overexpression in LX-2 and HHSC by flow cytometry and RTqPCR. **(A)** Gating strategy for flow sorting of lentivirally transduced cells. First, cells were selected (left panel) before gating on singlets (middle panel). Cells were then gated based on the 99 percent percentile of non-transduced cells to identify cells positive for GFP (right panel). Red polygons show gates and the red vertical line in the right panel shows the cut-off for GFP positivity. **(B)** Bar diagram showing percentage of GFP-positive cells in GREM1 or GFP-control lentivirally transduced LX-2, $n=1$. **(C)** SybrGreen RTqPCR results for GFP and GREM1 mRNA in lentivirally transduced LX-2, $n=4$. **(D)** Bar diagram showing percentage of GFP-positive cells in GREM1 or GFP-control lentivirally transduced HHSC, $n=3$. **(E)** SybrGreen RTqPCR results for GFP and GREM1 mRNA in lentivirally transduced HHSC, $n=3$. **(F)** Data in B and D are given as individual data points and mean \pm SD; data in C and E are given as individual data points and mean. * $P<0.05$, ** $P<0.01$ and *** $P<0.001$ in paired two-sided t-test.

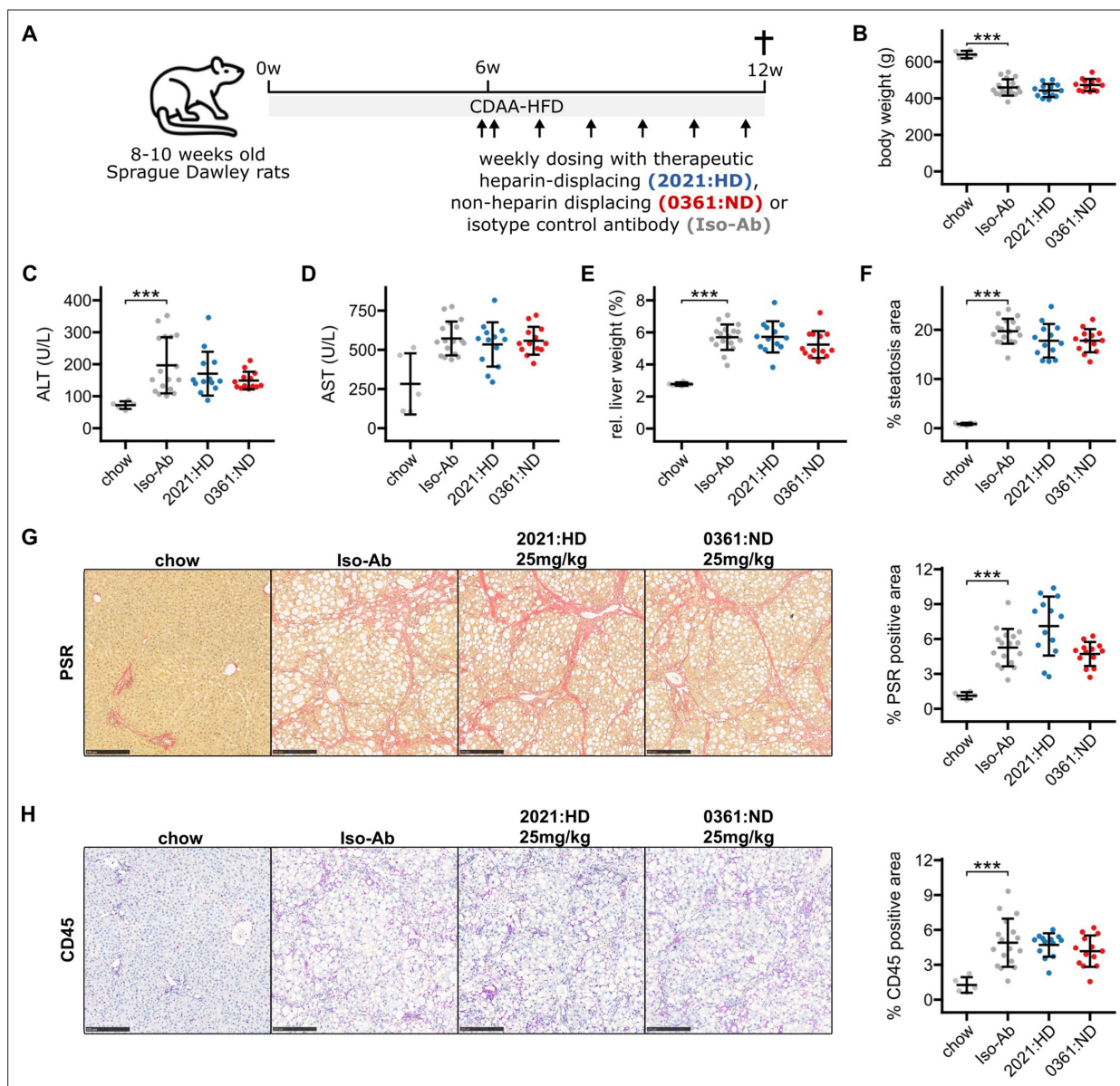


Figure 5. Results for anti-Gremlin-1 antibody treatment on CDAH-HFD induced MASH and fibrosis in rats. **(A)** Schematic showing the study design for the animal experiment. 8–12 weeks old Sprague Dawley rats were fed a choline-deficient, L-amino acid defined high fat diet (CDAH-HFD) or standard chow for 12 weeks and treated with weekly subcutaneous injections of heparin-displacing, non-heparin-displacing or isotype control antibodies for the last 6 weeks. **(B)** Quantification of body weight in grams at the end of the study. **(C)** Quantification of plasma alanine aminotransferase (ALT) in U/L. **(D)** Quantification of plasma aspartate aminotransferase (AST) in U/L. **(E)** Quantification of relative liver weight percent of total body weight. **(F)** Quantification of histological liver steatosis area in percent. Data are given as mean \pm SD for $n=5$ (chow), $n=17$ (Iso-Ab) and $n=13$ (2021 & 0361) animals per group. **(G)** Left panel shows representative histological images for picrosirius red staining for different treatment conditions. Scale bars represent 250 μ m. Right panel shows quantification of picrosirius red staining (PSR) in percent of total area. **(H)** Left panel shows representative histological images for CD45 IHC for different treatment conditions. Scale bars represent 250 μ m. Right panel shows quantification of CD45 IHC in percent of total area. Data are given as mean \pm SD for $n=5$ (chow), $n=17$ (Iso-Ab) and $n=13$ (2021 & 0361) animals per group. Significance was determined by multiple two-sided paired Welch t -tests against Iso-Ab, followed by Bonferroni-Holm adjustment ($***P<0.001$).

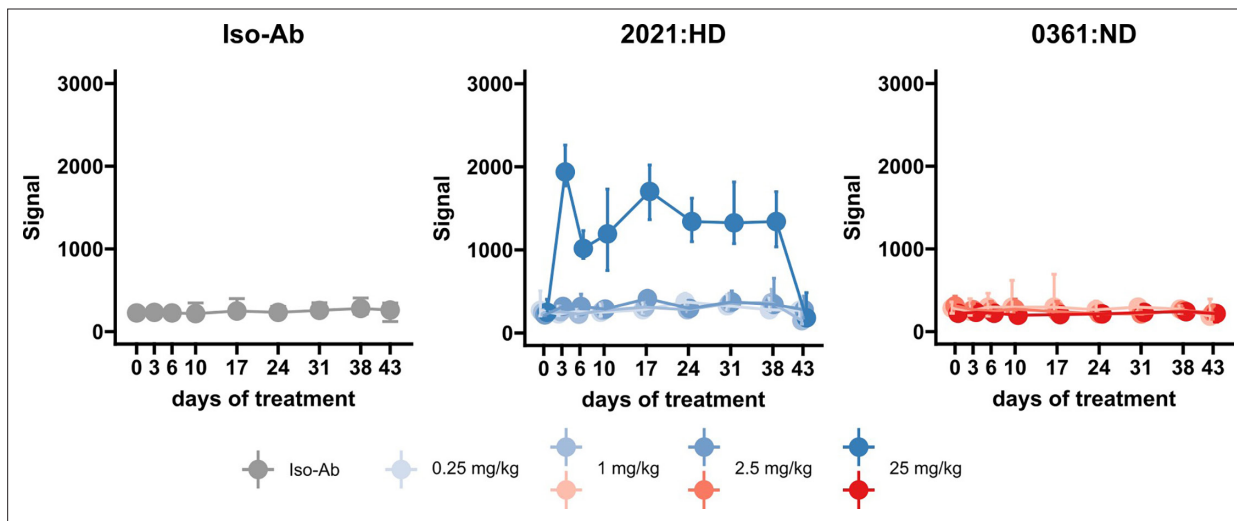


Figure 5—figure supplement 1. Target engagement studies in the rat CDA-HFD model. Peripheral blood samples were taken before first antibody injection and at different timepoints during treatment, as indicated on the x-axes. Plots show signal intensity for Gremlin-1 protein in plasma by alphaLISA. All data are given as median and IQR.

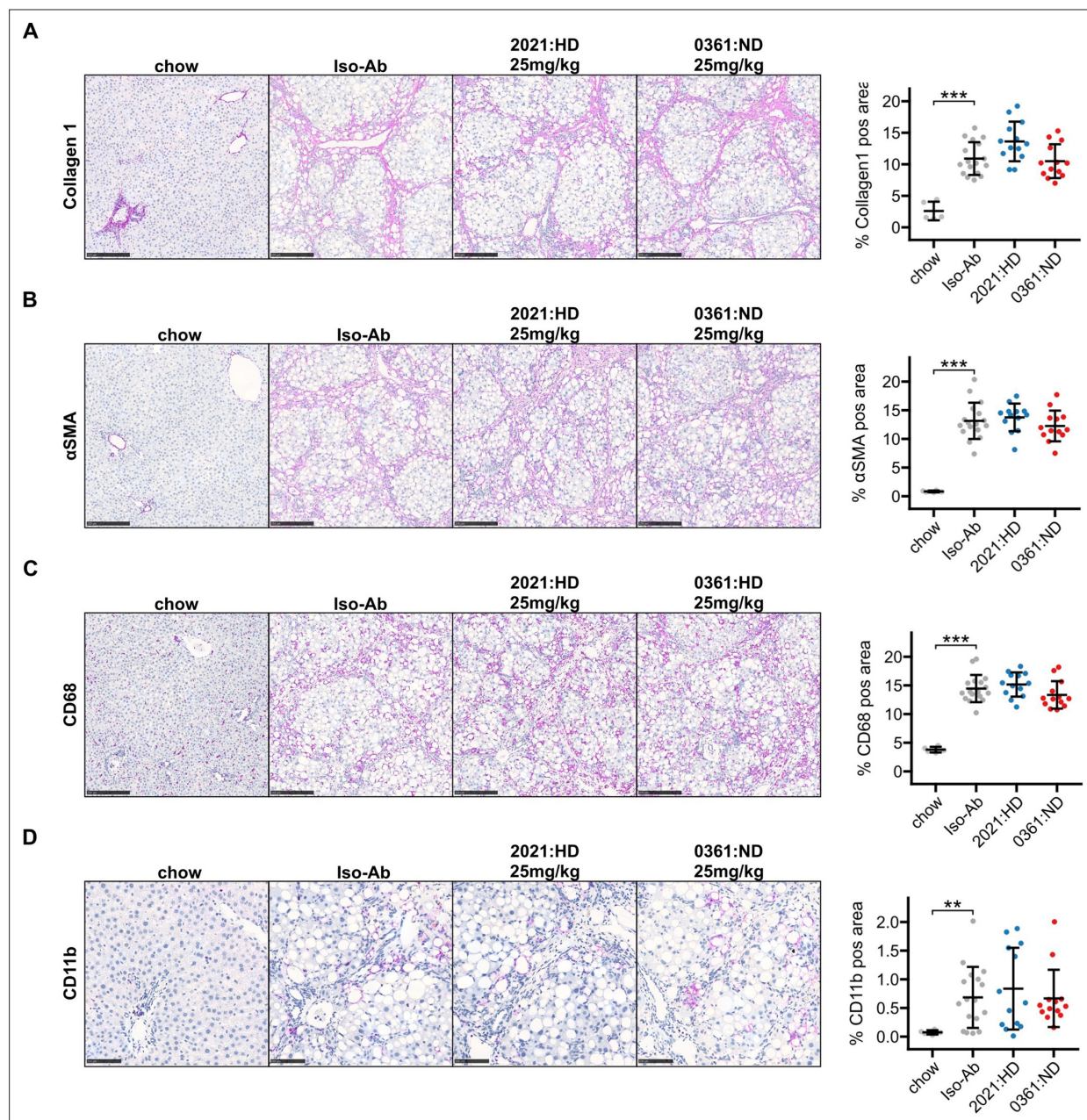


Figure 5—figure supplement 2. Additional IHC data from rat CDAA-HFD study. **(A)** Left panel shows representative histological images for Collagen 1 IHC for different treatment conditions. Scale bars represent 250 μ m. Right panel shows quantification of Collagen 1 staining in percent of total area. **(B)** Left panel shows representative histological images for alpha smooth muscle actin (α SMA) IHC for different treatment conditions. Scale bars represent 250 μ m. Right panel shows quantification of α SMA staining in percent of total area. **(C)** Left panel shows representative histological images for CD68 IHC for different treatment conditions. Scale bars represent 250 μ m. Right panel shows quantification of CD68 staining in percent of total area. **(D)** Left panel shows representative histological images for CD11b IHC for different treatment conditions. Scale bars represent 100 μ m. Right panel shows quantification of CD11b staining in percent of total area. Data are given as mean \pm SD for n=5 (chow), n=17 (Iso-Ab) and n=13 (2021 & 0361) animals per group. Significance was determined by multiple two-sided paired Welch t-tests against Iso-Ab, followed by Bonferroni-Holm adjustment (** P <0.01, *** P <0.001).

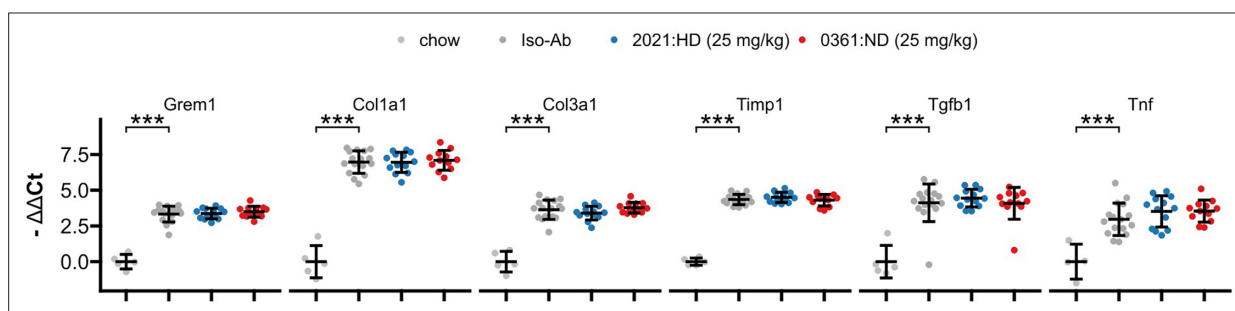


Figure 5—figure supplement 3. RTqPCR results for anti-Gremlin-1 antibody treatment on CDAA-HFD induced MASH and fibrosis in rats. Data are given as single data points and mean \pm SEM for $-\Delta\Delta C_t$ relative to chow control and normalised to B2m expression. *** $P < 0.001$ in One-Way ANOVA and post-hoc Dunnett test compared to Iso-Ab treated animals.

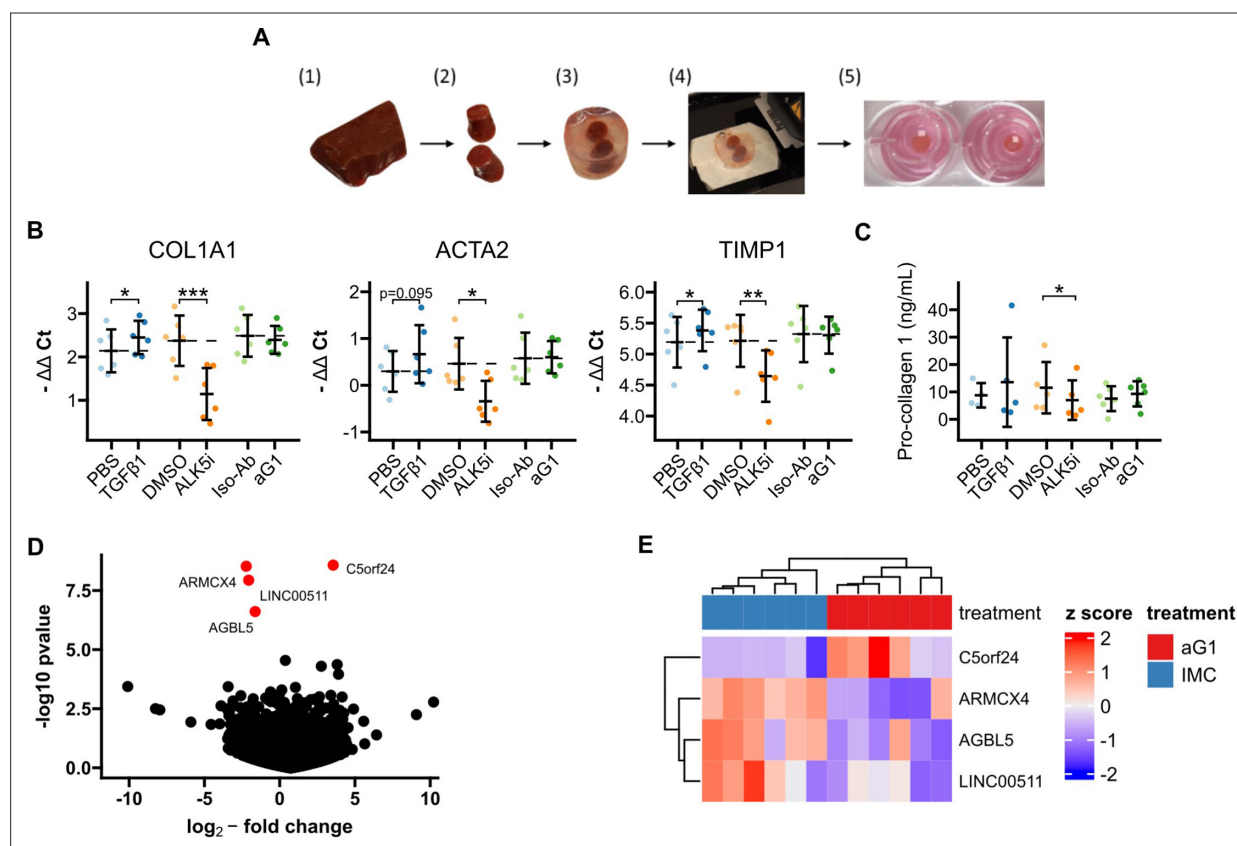


Figure 6. PCLS. **(A)** Schematic for generation of human cirrhotic PCLS. (Younossi et al., 2016) Human cirrhotic liver tissue was obtained from explants and (Younossi et al., 2018) 8 mm biopsy cores were taken. (Powell et al., 2021) Tissue samples were then embedded in low-melt agarose before (Taylor et al., 2020) being cut into 250 μm thin slices on a vibratome. (Church et al., 2017) Finally, slices were incubated in 8 μm 12-well inserts for 24 hours under constant agitation. **(B)** RTqPCR results for fibrogenic marker genes in cirrhotic PCLS. Data are given as individual data points and mean ± SD for -ΔΔ Ct relative to untreated control and normalised to the geometric mean of SRSF4, HPRT1, CTCF and ERCC expression. **P*<0.05, ***P*<0.01, ****P*<0.001 in One-Way ANOVA and post-hoc paired t-tests for pre-defined comparisons with Bonferroni-Holm adjustment. **(C)** Pro-collagen 1 protein levels in PCLS culture supernatants. Data are given as individual data points and mean ± SD. **P*<0.05 in One-Way ANOVA and post-hoc paired t-tests for pre-defined comparisons with Bonferroni-Holm adjustment. **(D)** Volcano plot of differential gene expression analysis of 3' QuantSeq mRNA sequencing showing log₂ -fold changes and the negative decadic logarithm of unadjusted p-values for all expressed genes in aG1 vs Iso-Ab treated PCLS. Significantly regulated genes (i.e. adj. *P*-value <0.05) are labelled and marked in red. **(E)** Heatmap showing centred and scaled gene expression for significantly regulated genes. The anti-Gremlin-1 antibody (aG1) used for experiments in panels B and C was the 0030:HD antibody.

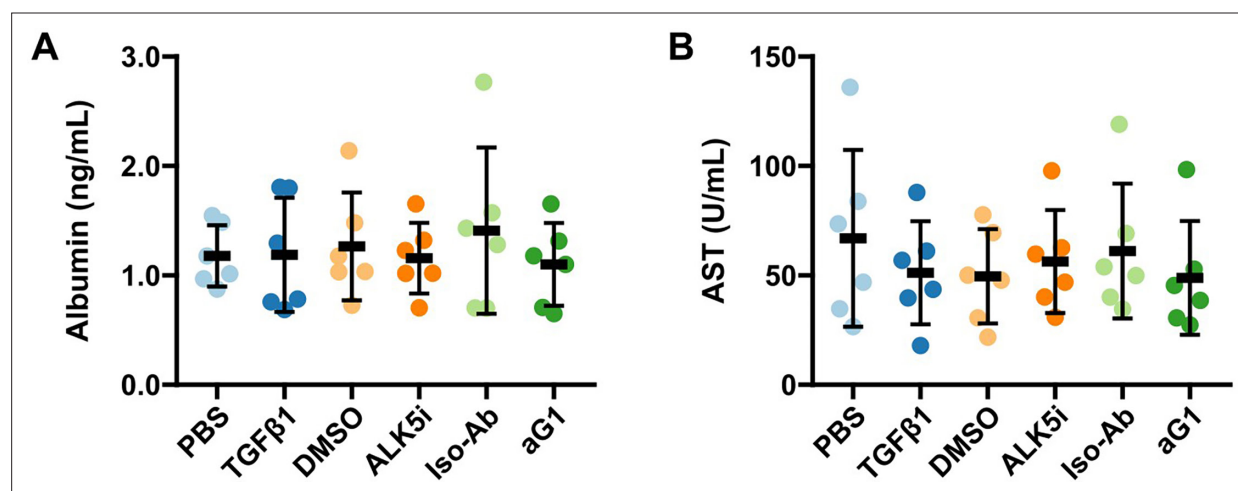


Figure 6—figure supplement 1. AST and Albumin levels in precision-cut liver slices supernatants. (A) Albumin levels in supernatants of treated PCLS. (B) AST enzymatic activity in supernatants of treated PCLS. The anti-Gremlin-1 antibody (aG1) used for experiments was the 0030:HD antibody. Data are given as individual data points (coloured points) and mean \pm SD for $n=6$ per treatment condition.

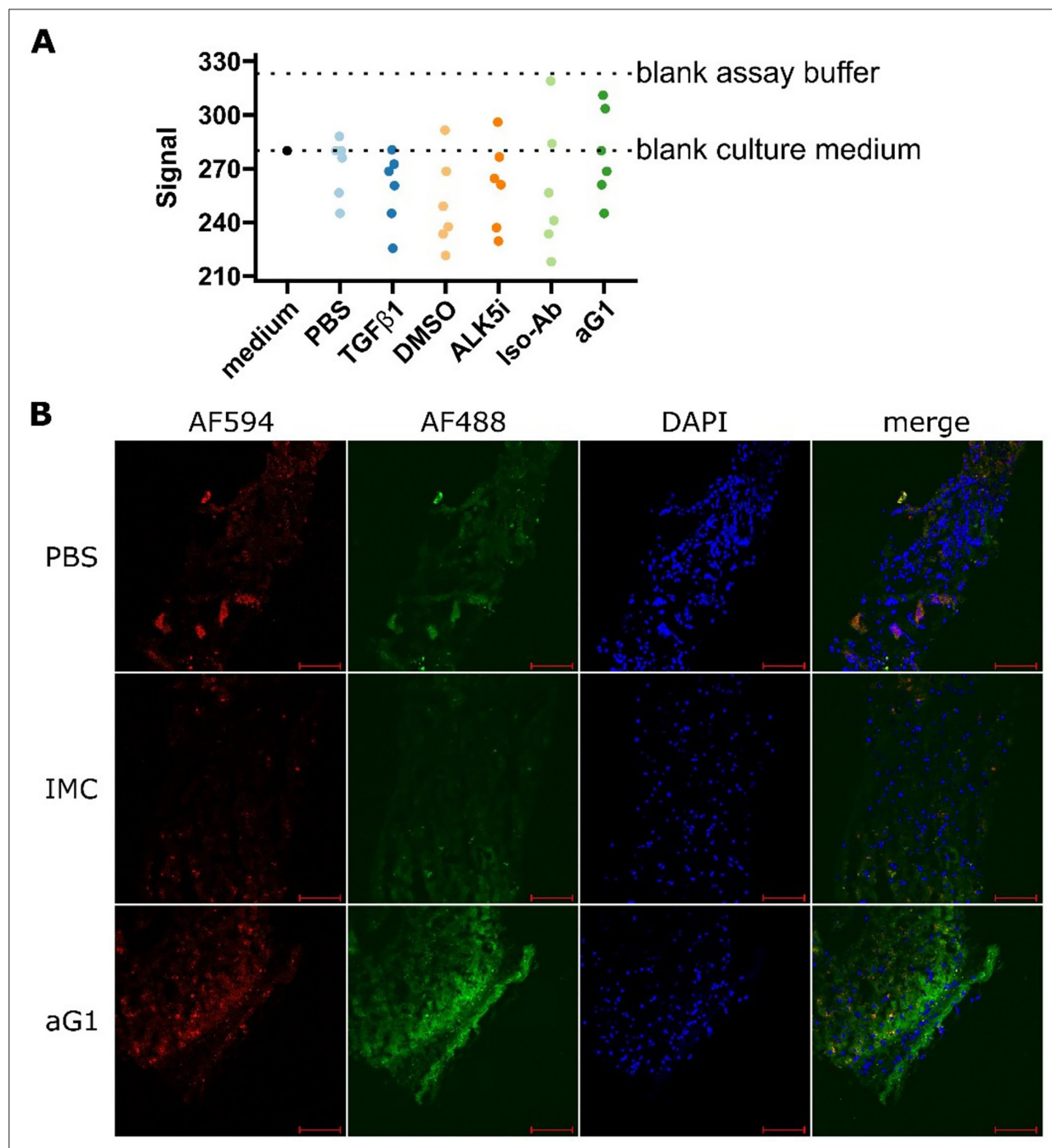


Figure 6—figure supplement 2. Target engagement studies in PCLS. **(A)** Results of alphaLISA for Gremlin-1 protein in supernatants of treated cirrhotic PCLS. Data are given as individual data points for fluorescent signal intensity and dotted lines indicate the signal intensities obtained using blank culture medium or blank assay buffer. **(B)** One set of cirrhotic PCLS was treated with either PBS or AF488-conjugated non-heparin displacing isotype control or anti-Gremlin-1 antibody for 24 h. Unfixed frozen sections were imaged after autofluorescence quenching and staining with DAPI. Red autofluorescence was detected using the AF594 channel. Scale bar represents 100 μ m. **(C)** The anti-Gremlin-1 antibody (aG1) used for experiments in panels A was the 0030:HD antibody, the aG1 used for B was the 0032:ND antibody.